

Response of temperature dependence of an elastic modulus in microstretch generalized thermoelasticity

Rajneesh Kumar[†] and Rajani Rani Gupta[‡]

Department of Mathematics, Kurukshetra University, Kurukshetra-136 119, India

(Received September 13, 2007, Accepted October 7, 2008)

Abstract. Laplace-Fourier transform techniques are used to investigate the interaction caused by mechanical, thermal and microstress sources in a generalized thermomicrostretch elastic medium with temperature-dependent mechanical properties. The modulus of elasticity is taken as a linear function of reference temperature. The integral transforms are inverted using a numerical technique to obtain the normal stress, tangential stress, tangential couple stress, microstress and temperature distribution. Effect of temperature dependent modulus of elasticity and thermal relaxation times have been depicted graphically on the resulting quantities. Comparisons are made with the results predicted by the theories of generalized thermoelasticity. Some particular cases are also deduced from the present investigation.

Keywords: Microstretch generalized thermoelastic solid, Integral transforms, Concentrated source, Microstress force

1. Introduction

The concept of microcontinuum, proposed by Eringen (1999), can take into account the microstructure effects while the theory itself is still a continuum formulation. The first grade microcontinuum consists a hierarchy of theories, namely, micropolar, microstretch and micromorphic, depending on how much microdegrees of freedom are incorporated. These high order continuum theories are considered to be potential tools to model the behavior of the material with a complicated microstructure. For example, in the case of a foam composite, when the size of the reinforced phase is comparable to the intrinsic length scale of the foam. In these situations, the microstructure of the foam must be taken into account to some degree, so a high order continuum model must be assigned for the foam matrix. The same remains true for nanocomposites, since the scale of the reinforced phase is so small, the surroundings matrix cannot be homogenized as a simple material (Cauchy medium), some intrinsic microstructures of the matrix must be considered in a proper continuum model. Microstretch theory is a generalization of the theory of micropolar elasticity and a special case of the micromorphic theory. The microstretch solids are those in which material particles can undergo stretches (expansion and contraction) in addition to translation and rotation. Thus a microstretch elastic solid possesses seven degrees of freedom: three for translation,

[†] Ph.D., Corresponding author, E-mail: rajneesh_kuk@rediffmail.com

[‡] E-mail: rajani_gupta_83@yahoo.com

three for rotation (as in micropolar elasticity) and one for stretch, required by substructures. Such a generalized media can catch more detailed information about the microdeformation inside a material point, which is more suitable for modelling the overall property of the foam matrix in the case of foam composites. Kumar and Singh (1998) studied wave propagation in a generalized thermomicrostretch elastic solid. De Cicco (2003) investigated the stress concentration effects in microstretch elastic bodies. Liu and Hu (2004) investigated the inclusion problem of microstretch. Svanadze (2004) constructed fundamental solution of the system of equations of steady oscillations in the theory of microstretch elastic solids. Bakshi *et al.* (2007) investigated the problem of wave propagation in materials with memory in generalized thermoelasticity. The elastic modulus is an important physical property of materials reflecting the elastic deformation capacity of the material when subjected to an applied external load. Most of the investigations were done under the assumption of the temperature-independent material properties, which limit the applicability of the solutions obtained to certain ranges of temperature. Modern structural elements are often subjected to temperature change of such magnitude that their material properties may no longer be regarded as having constant values even in an approximate sense. At high temperature the material characteristics such as the modulus of elasticity, coefficient of thermal expansion and thermal conductivity etc. are no longer constants. The thermal and mechanical properties of the materials vary with temperature, so the temperature-dependence of the material properties must be taken into consideration in the thermal stress analysis of these elements. Tanigawa (1995) investigated thermoelastic problems for non-homogeneous structural material. Ezzat *et al.* (2001, 2004) investigated the dependence of modulus of elasticity on reference temperature in generalized thermoelasticity and obtained interesting results. Motivated by the recent experimental studies (1973, 1976, 1999, 2003) showing the necessity of taking into consideration the real behavior of the material characteristics, this paper presents an attempt to examine the temperature dependency of elastic modulus on the behavior of two-dimensional solutions in a generalized thermo-microstretch elastic medium. The physical applications are encountered in the context of problems such as ground explosions and oil industries. This problem is useful in the field of geomechanics, where interest is in various phenomenon occurring in earthquakes and measurements of stresses and temperature distribution due to presence of certain sources.

2. Basic equations

The basic equations in linear homogeneous, isotropic microstretch generalized thermoelastic solid in the absence of body forces, body couples, stretch force and heat sources are given by

2.1. Balanced Laws

Balance of Momentum

$$t_{kl,k} = \rho \ddot{u}_l \quad (1)$$

Balance of Moment of Momentum

$$m_{kl,k} + \varepsilon_{lmn} t_{mn} = \rho j \ddot{\phi}_m \quad (2)$$

Balance of first stress moments

$$\lambda_{k,k}^* + (t-s) = \rho j_0 \ddot{\phi}^* \quad (3)$$

Energy Equation

$$\rho \dot{\eta} T_0 = q_{i,i} \tag{4}$$

2.2. Constitutive Relations

$$t_{kl} = \lambda u_{r,r} \delta_{kl} + \mu (u_{l,k} + u_{k,l}) + K(u_{l,k} - \epsilon_{klr} \phi_r) + \lambda_0 \delta_{kl} \phi^* - \nu \left(1 + \tau_1 \frac{\partial}{\partial t}\right) \delta_{kl} T, \tag{5}$$

$$m_{kl} = \alpha \phi_{r,r} + \beta \phi_{k,l} + \gamma \phi_{l,k} + b_0 \epsilon_{mlk} \phi^*_{,m}, \tag{6}$$

$$\lambda^*_k = \alpha_0 \phi^*_{,k} + b_0 \epsilon_{klm} \phi_{l,m}, \tag{7}$$

$$s - t = \lambda_0 u_{k,k} + \lambda_1 \phi^* - \beta_1 T, \tag{8}$$

$$q_k = K \delta_{kl} T_{,k}, \tag{9}$$

$$\left. \begin{aligned} \rho \eta T_0 &= \nu T_0 u_{k,k} + \nu_1 T_0 \phi^* + \rho C^* T \\ \left(1 + \tau_0 \frac{\partial}{\partial t}\right) q_{i,i} &= K^* T_{i,i} \end{aligned} \right\}, \text{ for L-S Theory} \tag{10}$$

and

$$\left. \begin{aligned} \rho \eta T_0 &= \nu T_0 u_{k,k} + \nu_1 T_0 \phi^* + \rho C^* \left(\frac{\partial}{\partial t} + \tau_0 \frac{\partial^2}{\partial t^2}\right) T \\ q_{i,i} &= K^* T_{i,i} \end{aligned} \right\}, \text{ for G-L Theory} \tag{11}$$

Substituting the value from Eqs. (5)-(11) in Eqs. (1)-(4), we obtain

$$(\lambda + 2\mu + K) \nabla(\nabla \cdot \vec{u}) - (\mu + K) \nabla \times \nabla \times \vec{u} + K \nabla \times \vec{\phi} + \lambda_0 \nabla \phi^* - \nu \left(1 + \tau_1 \frac{\partial}{\partial t}\right) \nabla T = \rho \frac{\partial^2 \vec{u}}{\partial t^2}, \tag{12}$$

$$(\alpha + \beta + \gamma) \nabla(\nabla \cdot \vec{\phi}) - \gamma \nabla \times \nabla \times \vec{\phi} + K \nabla \times \vec{u} - 2K \vec{\phi} = \rho j \frac{\partial^2 \vec{\phi}}{\partial t^2}, \tag{13}$$

$$\alpha_0 \nabla^2 \phi^* + \nu_1 \left(1 + \tau_1 \frac{\partial}{\partial t}\right) T - \lambda_1 \phi^* - \lambda_0 \nabla \cdot \vec{u} = \rho j_0 \frac{\partial^2 \phi^*}{\partial t^2}, \tag{14}$$

$$K^* \nabla^2 T = \rho C^* \left(\frac{\partial}{\partial t} + \tau_0 \frac{\partial^2}{\partial t^2}\right) T + \nu T_0 \left(\frac{\partial}{\partial t} + n_0 \tau_0 \frac{\partial^2}{\partial t^2}\right) \nabla \cdot \vec{u} + \nu_1 T_0 \left(\frac{\partial}{\partial t} + n_0 \tau_0 \frac{\partial^2}{\partial t^2}\right) \phi^*, \tag{15}$$

where list of symbols are given in Appendix A.

3. Formulation and solution of the problem

We considered a microstretch generalized thermoelastic medium with temperature dependent elastic modulus. The rectangular Cartesian coordinate system (x, y, z) with z axis pointing vertically into the medium is introduced. For the two dimensional problem, we assume the components of the displacement \vec{u} and microrotation vector $\vec{\phi}$, of the form

$$\vec{u} = (u, 0, w), \quad \vec{\phi} = (0, \phi_2, 0), \tag{16}$$

We assume temperature dependent elastic constants of the form

$$(\lambda, \lambda_0, \alpha, \beta, \mu, \nu, K, K^*, \gamma, \nu_1, b_0) = (\lambda_a, \lambda_{0a}, \alpha_a, \beta_a, \mu_a, \nu_a, K_a, K_a^*, \gamma_a, \nu_{1a}, b_{0a}) (1 - \alpha^* T_0), \quad (17)$$

where, α^* is called the empirical material constant. Also we define the dimensionless variables by the expressions

$$(x', z') = \frac{\omega^*}{c_1} (x, z), \quad (u', w') = \frac{\rho c_1 \omega^*}{\nu_a T_0} (u, w), \quad (\phi'_2, \phi^*) = \frac{\rho c_1^2}{\nu_a T_0} (\phi_2, \phi^*), \quad t'_{ij} = \frac{t_{ij}}{\nu_a T_0},$$

$$(m'_{ij}, \lambda'_i) = \frac{\omega^*}{c_1 \nu_a T_0} (m_{ij}, \lambda_i), \quad T = \frac{T}{T_0}, \quad t = \omega^* t, \quad (\tau'_0, \tau'_1) = \omega^* (\tau_0, \tau_1),$$

where

$$\omega^* = \frac{\rho C_1^* c_1^2}{K_a^*}, \quad \rho c_1^2 = \lambda_a + 2\mu_a + K_a \quad (18)$$

where ω^* is the characteristic frequency of the material and C_1 is the longitudinal wave velocity of the medium.

The displacement components, $u(x, z, t)$ and $w(x, z, t)$, may be written in terms of the potential functions, $q(x, z, t)$ and $\psi(x, z, t)$, as

$$u = \frac{\partial q}{\partial x} + \frac{\partial \psi}{\partial z}, \quad w = \frac{\partial q}{\partial z} - \frac{\partial \psi}{\partial x}. \quad (19)$$

and Laplace and Fourier Transform defined as

$$\tilde{f}(x, y, p) = \int_0^\infty f(x, y, t) e^{-pt} dt, \quad (20)$$

and

$$\tilde{f}(\xi, y, p) = \int_{-\infty}^\infty \tilde{f}(x, y, t) e^{t\xi x} dx \quad (21)$$

Using Eqs. (16)-(21) in Eqs. (12)-(15), we obtain

$$\left(\frac{d^2}{dz^2} - \xi^2 - p^2 R \right) \tilde{q} + \frac{\lambda_{0a}}{\rho c_1^2} \tilde{\phi}^* - (1 + \tau_1 p) \tilde{T} = 0, \quad (22)$$

$$\left[\frac{(\mu_a + K_a)}{\rho c_1^2} \left(\frac{d^2}{dz^2} - \xi^2 \right) - p^2 R \right] \tilde{\psi} - \frac{K_a}{\rho c_1^2} \tilde{\phi}_2 = 0, \quad (23)$$

$$\left[\frac{d^2}{dz^2} - \xi^2 - \frac{2K_a c_1^2}{\gamma_a \omega^{*2}} \right] \tilde{\phi}_2 + \left[\frac{K_a c_1^2}{\gamma_a \omega^{*2}} \left(\frac{d^2}{dz^2} - \xi^2 \right) - \frac{\rho j c_1^2 p^2 R}{\gamma_a} \right] \tilde{\psi} = 0, \quad (24)$$

$$\left[\frac{\omega^{*2} \alpha_{0a}}{\rho c_1^4} \left(\frac{d^2}{dz^2} - \xi^2 \right) - \frac{\lambda_{1a}}{\rho c_1^2} - \frac{\rho j_0 \omega^{*2} p^2 R}{2\rho c_1^2} \right] \tilde{\phi}^* - \frac{\lambda_{0a}}{\rho c_1^2} \left(\frac{d^2}{dz^2} - \xi^2 \right) \tilde{q} + \frac{\nu_{1a}}{\nu_a} (1 + \tau_1 p) \tilde{T} = 0, \quad (25)$$

$$\varepsilon_1 (p + n_0 \tau_0 p^2) \left(\frac{d^2}{dz^2} - \xi^2 \right) \tilde{q} + \varepsilon_2 (p + n_0 \tau_0 p^2) \tilde{\phi}^* - \left(\frac{d^2}{dz^2} - \xi^2 - (p + \tau_0 p^2) R \right) \tilde{T} = 0. \quad (26)$$

Solving Eqs. (22), (25) and (26), we obtain

$$\left[\frac{d^6}{dz^6} + C \frac{d^4}{dz^4} + D \frac{d^2}{dz^2} + E \right] (\tilde{q}, \tilde{\phi}^*, \tilde{T}) = 0, \quad (27)$$

and after solving Eqs. (23) and (24), we obtain

$$\left[\frac{d^4}{dz^4} + A \frac{d^2}{dz^2} + B \right] (\tilde{\psi}, \tilde{\phi}_2) = 0, \tag{28}$$

where A, B, C, \dots are given in Appendix B.

The solution of Eqs. (27) and (28) satisfying the radiation condition that $\tilde{q}, \tilde{\phi}^*, \tilde{T}, \tilde{\psi}$ and $\tilde{\phi}_2 \rightarrow 0$ as $z \rightarrow \infty$ are given by

$$\begin{aligned} \tilde{\psi} &= A_1 e^{-q_1 z} + A_2 e^{-q_2 z}, & \tilde{\phi}_2 &= A_1 m_1 e^{-q_1 z} + A_2 m_2 e^{-q_2 z} \\ \tilde{q} &= A_3 e^{-q_3 z} + A_4 e^{-q_4 z} + A_5 e^{-q_5 z}, & \tilde{\phi}^* &= A_3 r_3 e^{-q_3 z} + A_4 r_4 e^{-q_4 z} + A_5 r_5 e^{-q_5 z}, \\ \tilde{T} &= A_3 s_3 e^{-q_3 z} + A_4 s_4 e^{-q_4 z} + A_5 s_5 e^{-q_5 z}, \end{aligned} \tag{29}$$

where, m_1, m_2, \dots are given in Appendix C.

4. Boundary conditions

The boundary conditions on the surface $z = 0$ are given by

$$\begin{aligned} \text{(i)} \quad & t_{33} = -P_1 \zeta(x) \delta(t), \\ \text{(ii)} \quad & t_{31} = -P_2 \zeta(x) \delta(t), \\ \text{(iii)} \quad & m_{32} = -P_3 \zeta(x) \delta(t), \\ \text{(iv)} \quad & T = P_4 \zeta(x) \delta(t), \\ \text{(v)} \quad & \lambda_3^* = -P_5 \zeta(x) \delta(t), \end{aligned} \tag{30}$$

where P_1, P_2, P_3, P_5 are the magnitudes of applied forces, P_4 is the constant temperature applied at the boundary and $\zeta(x)$ is the known function defined later. Applying the Laplace and Fourier transform defined by (20) and (21) on boundary conditions (30) and with the help of Eq. (29), we obtain the components of normal force stress, tangential force stress, tangential couple stress, temperature distribution and microstress as

$$\tilde{t}_{33} = \frac{R^{-1}}{\Delta} (\Delta_1 a_1^* e^{-q_1 z} + \Delta_2 a_2^* e^{-q_2 z} + \Delta_3 a_3^* e^{-q_3 z} + \Delta_4 a_4^* e^{-q_4 z} + \Delta_5 a_5^* e^{-q_5 z}), \tag{31}$$

$$\tilde{t}_{31} = \frac{R^{-1}}{\Delta} (\Delta_1 b_1^* e^{-q_1 z} + \Delta_2 b_2^* e^{-q_2 z} + \Delta_3 b_3^* e^{-q_3 z} + \Delta_4 b_4^* e^{-q_4 z} + \Delta_5 b_5^* e^{-q_5 z}), \tag{32}$$

$$\tilde{m}_{32} = \frac{R^{-1}}{\Delta} (\Delta_1 c_1^* e^{-q_1 z} + \Delta_2 c_2^* e^{-q_2 z} + \Delta_3 c_3^* e^{-q_3 z} + \Delta_4 c_4^* e^{-q_4 z} + \Delta_5 c_5^* e^{-q_5 z}), \tag{33}$$

$$\tilde{\lambda}_3^* = \frac{R^{-1}}{\Delta} (\Delta_1 d_1^* e^{-q_1 z} + \Delta_2 d_2^* e^{-q_2 z} + \Delta_3 d_3^* e^{-q_3 z} + \Delta_4 d_4^* e^{-q_4 z} + \Delta_5 d_5^* e^{-q_5 z}), \tag{34}$$

$$\tilde{T} = \frac{R^{-1}}{\Delta} (\Delta_3 s_3 e^{-q_3 z} + \Delta_4 s_4 e^{-q_4 z} + \Delta_5 s_5 e^{-q_5 z}), \tag{35}$$

where $\Delta, \Delta_1, \Delta_2$ etc. are defined in Appendix D.

Case I – Normal Stress

To obtain the expressions due to normal stress we must set $P_1 = 1$ and $P_2 = P_3 = P_4 = P_5 = 0$ in the boundary condition (30).

Case II – Tangential Stress

To obtain the expressions due to tangential stress we must set $P_2 = 1$ and $P_1 = P_3 = P_4 = P_5 = 0$ in the boundary condition (30).

Case III – Tangential Couple Stress

To obtain the expressions due to tangential couple stress we must set $P_3 = 1$ and $P_1 = P_2 = P_4 = P_5 = 0$ in the boundary condition (30).

Case IV – Thermal Source

To obtain the expressions due to thermal source we must set $P_4 = 1$ and $P_1 = P_2 = P_3 = P_5 = 0$ in the boundary condition (30).

Case V – Microstress Force

To obtain the expressions due to microstress force we must set $P_5 = 1$ and $P_1 = P_2 = P_3 = P_4 = 0$ in the boundary condition (30).

5. Application*Case – I : Concentrated Source*

To determine normal stress, tangential stress, tangential couple stress and temperature distribution due to concentrated force described by Dirac delta function $\zeta(x) = \delta(x)$ must be used with

$$\tilde{\zeta}(\xi) = 1 \quad (36)$$

Case – II : Distributed Source

The solution due to force distributed over a strip dimensionless width $2a$, applied on the half space is obtained by setting

$$\zeta(x) = H(x + a) - H(x - a) \quad (37)$$

in Eq. (30). Using the Eq. (18) and then applying Laplace and Fourier transforms defined by Eqs. (20) and (21) on Eq. (37) we obtain

$$\tilde{\zeta}(\xi) = \frac{2\sin(\xi a)}{\xi} \quad (38)$$

The expressions for stresses and temperature distribution can be obtained for concentrated and uniformly distributed source by replacing $\tilde{\zeta}(\xi)$ from (36) and (38) in Eqs. (31)-(35).

Particular Cases

(i) If we take $\tau_1 = 0, n_0 = 1$, in Eqs. (31)-(35), we obtain the corresponding expressions of stresses and temperature distribution for L-S theory.

(ii) If we take $\tau_1 > 0, n_0 = 0$, in Eqs. (31)-(35), the corresponding expressions of stresses and temperature distribution are obtained for G-L theory.

(iii) Taking $\tau_0 = \tau_1 = 0$, in Eqs. (31)-(35), yield the corresponding expressions of stresses and temperature distribution for Coupled theory of thermoelasticity.

Special Case

If we take $R = 1$, in Eqs. (31)-(35), we obtain the corresponding expressions of stresses and temperature distribution for thermomicrostretch elastic solid. These results tally with the one obtained by Kumar *et al.* (2000) in the case of concentrated mechanical source by changing the suitable parameters.

6. Inversion of the transform

The transformed stresses and temperature distribution are functions of $z, \tilde{\zeta}$, the parameters of Laplace and Fourier transforms p and ξ , respectively, and hence are of the form $f(\xi, z, p)$. To obtain the solution of the problem in the physical domain, first we invert the Fourier transform and then Laplace transform by using the method applied by Kumar *et al.* (2004).

7. Numerical results and discussion

We take the case of magnesium crystal (1984) as a material subject to thermal disturbance for numerical calculations. The physical constants used by us are

$$\begin{array}{lll} \rho = 1.74 \text{ kg/m}^3, & j = 0.2 \times 10^{-15} \text{ m}^2, & \lambda = 9.4 \times 10^{11} \text{ N/m}^2, \\ \mu = 4.0 \times 10^{11} \text{ N/m}^2, & K = 1.0 \times 10^{11} \text{ N/m}^2, & \gamma = 0.779 \times 10^{-4} \text{ N/m}^2, \\ \lambda_0 = 0.5 \times 10^{11} \text{ N/m}^2, & \lambda_1 = 0.5 \times 10^{11} \text{ N/m}^2, & \alpha_0 = 0.779 \times 10^{-9} \text{ N/m}^2, \\ K^* = 0.6 \times 10^{-2} \text{ J/m sec } ^\circ\text{C}, & C^* = 0.23 \text{ J/Kg } ^\circ\text{C}, & T = 298 \text{ K}. \end{array}$$

The computations were carried out for a single value of time $t = 0.2$ and on the surface of the plane $z = 0$. The numerical values for the normal stress t_{33} , tangential couple stress m_{32} , temperature distribution T and microstress λ_3 on the surface of plane due to applied concentrated and uniformly distributed normal sources are shown in Figs. 1-24. In these figures the solid line with or without center symbol represents the solution obtained when modulus of elasticity is taken as a linear function of reference temperature ($TD, \alpha = .05$), while the dotted lines with or without center symbol represent the solution obtained in the case of temperature independent modulus of elasticity ($TI, \alpha^* = 0$). The comparison of three theories of generalized thermoelasticity, namely, Coupled

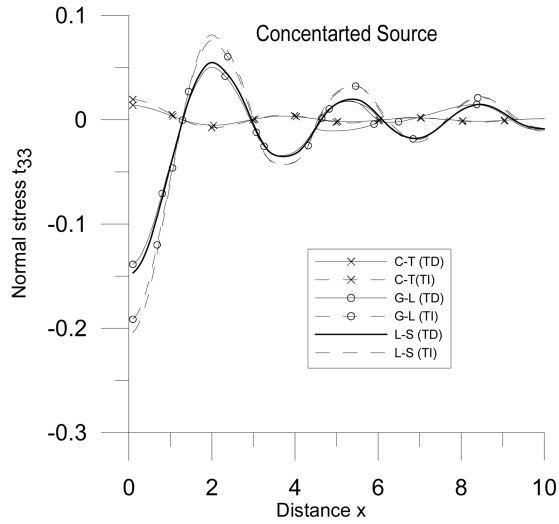


Fig. 1 Variation of normal stress with distance x

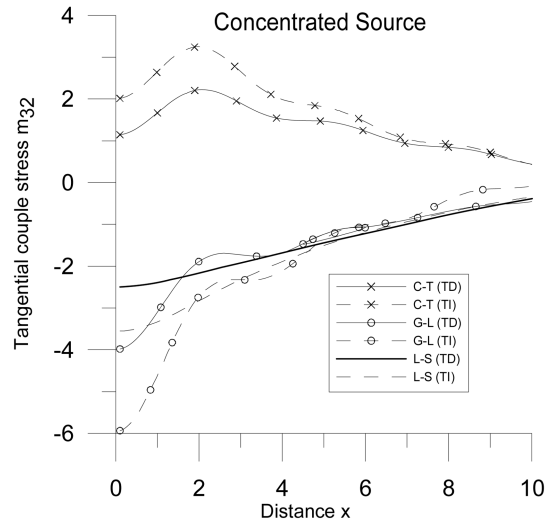


Fig. 2 Variation of tangential couple stress with distance x

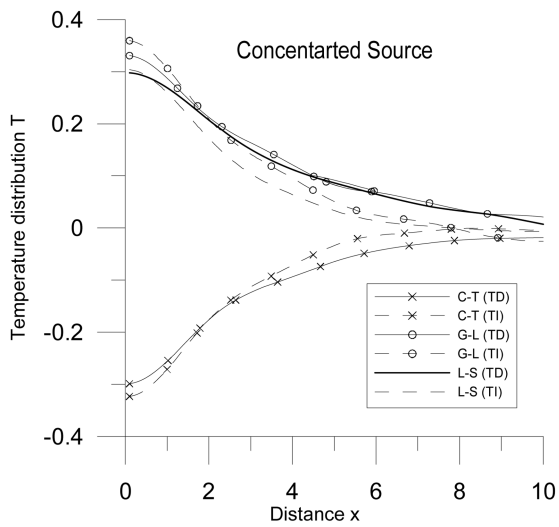


Fig. 3 Variations of temperature distribution T with distance x

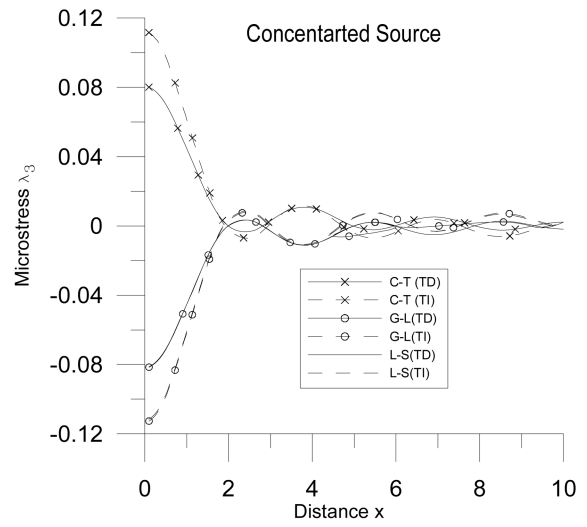


Fig. 4 Variations of microstress with distance x

thermoelasticity (C-T), Lord Shulman (L-S) and Green Lindsay (G-L) have been shown in all the graphs. The solid and dotted line with center symbol ($-x-x-$) corresponds to C-T theory, solid and dotted line with center symbol ($-o-o-$) corresponds to G-L theory and the solid and dotted line without center symbol correspond to the case of L-S theory. Figs. 1-4 shows the variation of normal stress, tangential couple stress, temperature distribution and microstress on application of concentrated mechanical force. It is observed from Fig. 1 that the value of normal force stress t_{33} for C-T theory initially decreases in the range $2 \leq x \leq 4$ and then oscillates with very small amplitude about origin, whereas for L-S and G-L theories its value start with sharp initial increase in the range $0 \leq x \leq 2$ then decreases in the range $2 \leq x \leq 3.5$ and then oscillate with decreasing

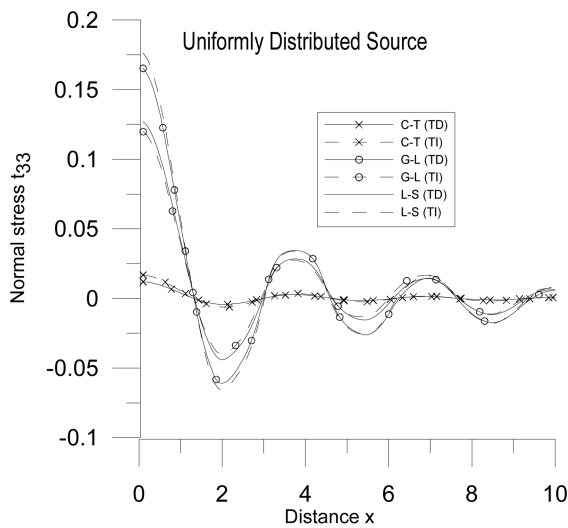


Fig. 5 Variations of normal stress with distance x

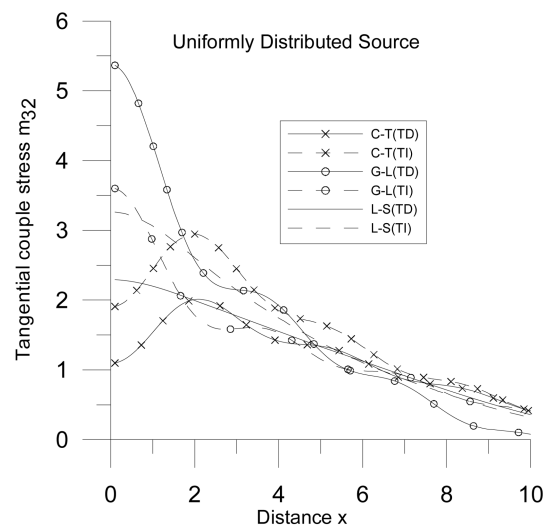


Fig. 6 Variation of tangential couple stress with distance x

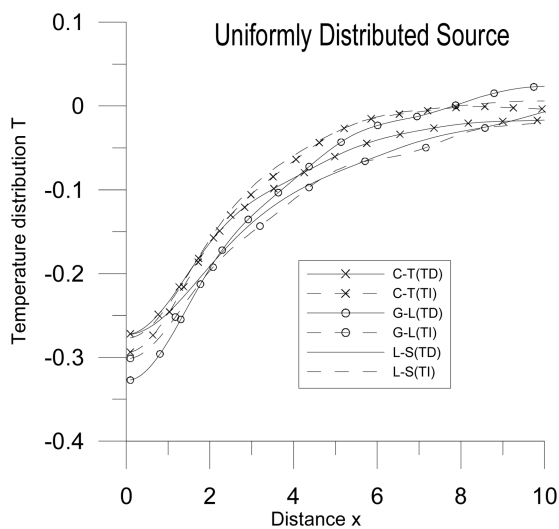


Fig. 7 Variation of Temperature Distribution T with distance x

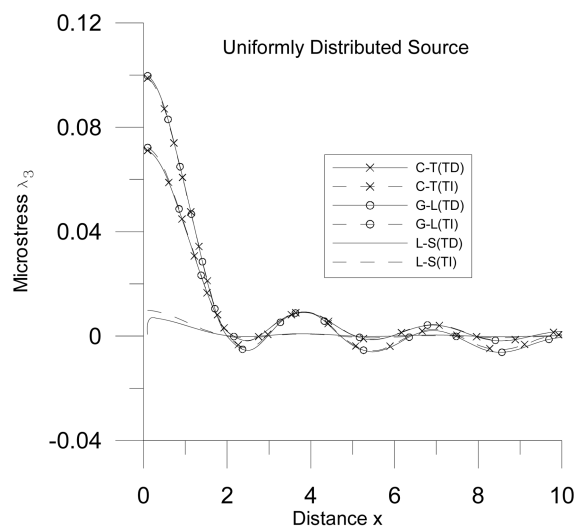


Fig. 8 Variations of microstress with distance x

amplitude. It is evident from Fig. 2 that the value of tangential couple stress m_{32} , for C-T theory start with initial increase then decreases with further increase in distance x , while for L-S and G-L theories its values increases with increase in x . Fig. 3 shows the variation of temperature distribution T , with distance x . For C-T theory the values of T increase with increase in distance x . However for L-S and G-L theories its values decrease with increase in distance x . It is evident from Fig. 4 that the values of microstress, λ_3 for C-T theory start with sharp decrease, then oscillate with small magnitude about origin, while reverse behavior is observed in the case of L-S and G-L theories. To show the comparison, in Fig. 4 the values for L-S theory is shown by dividing the original value by 10. Figs. 5-8 shows the variation of stresses and temperature distribution on application of

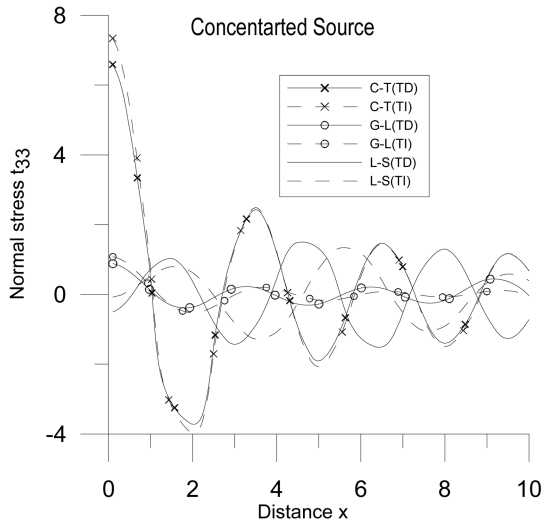


Fig. 9 Variations of normal stress with distance x

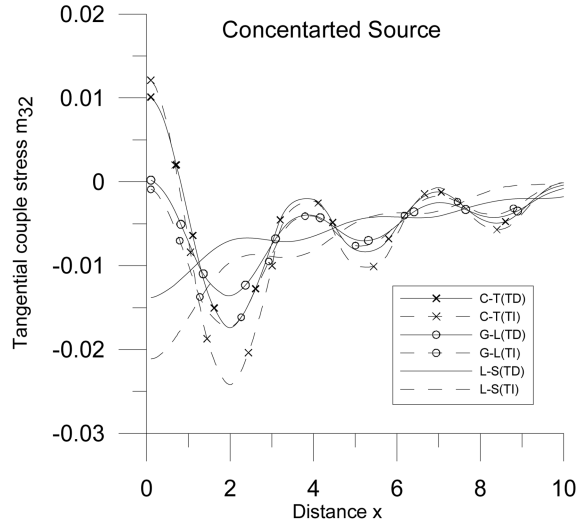


Fig. 10 Variation tangential couple stress with distance x

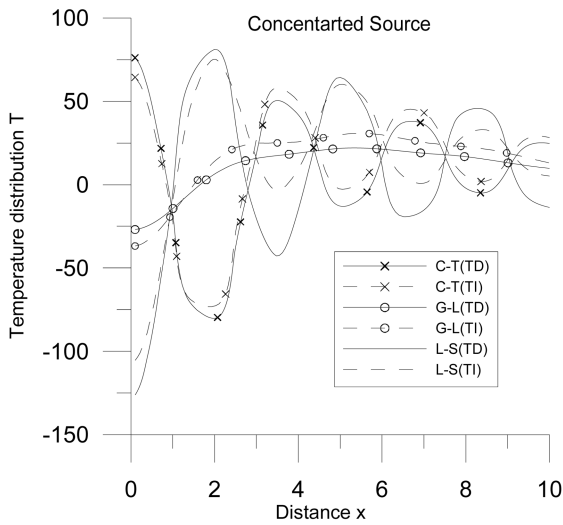


Fig. 11 Variation of temperature distribution T with distance x

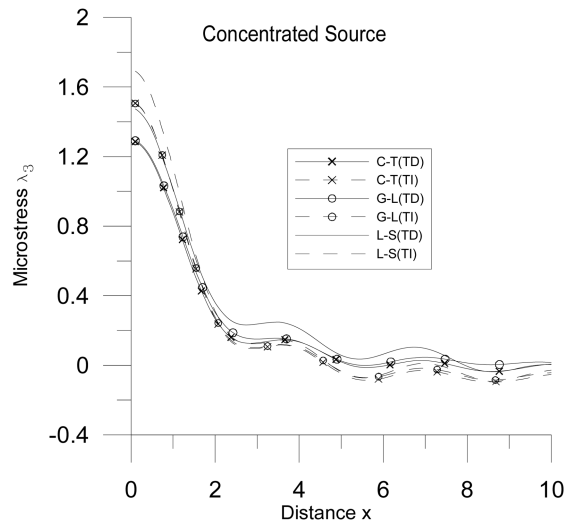


Fig. 12 Variation of microstress with distance x

uniformly distributed mechanical force. It is observed from Fig. 5 that the variation of t_{33} for C-T theory is same as on the application of concentrated force but that for L-S and G-L theories opposite behavior is observed. The values of m_{32} for both L-S and G-L theories, decrease with increase in distance x , while for C-T theory its values initially increase and then decrease with further increase in x , which is observed in Fig. 6. Fig. 7 shows that the values of T increase with increase in distance x for all the three theories of generalized thermoelasticity. To show the comparison, the values for L-S theory in Fig. 8 is shown by dividing the original value by 10. Also it is evident from Fig. 8 that the values of λ_3 start with sharp initial decrease, then oscillate about origin with very small amplitude for all the three theories all generalized thermoelasticity. Figs. 9-16

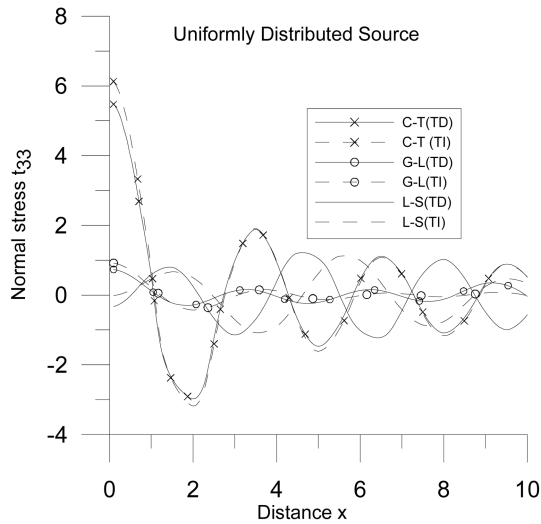


Fig. 13 Variations of normal stress with distance x

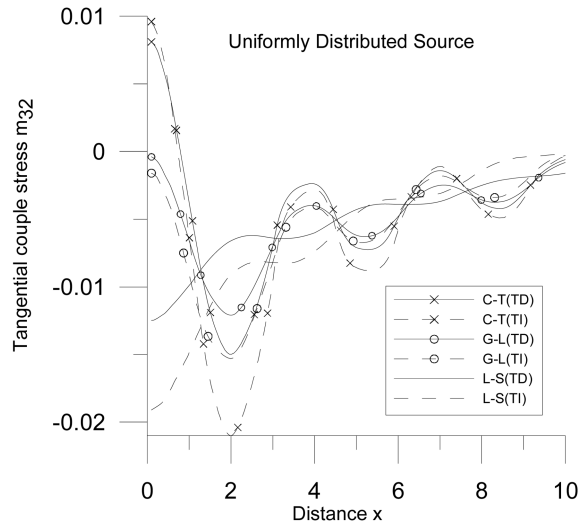


Fig. 14 Variation of tangential couple stress with distance x

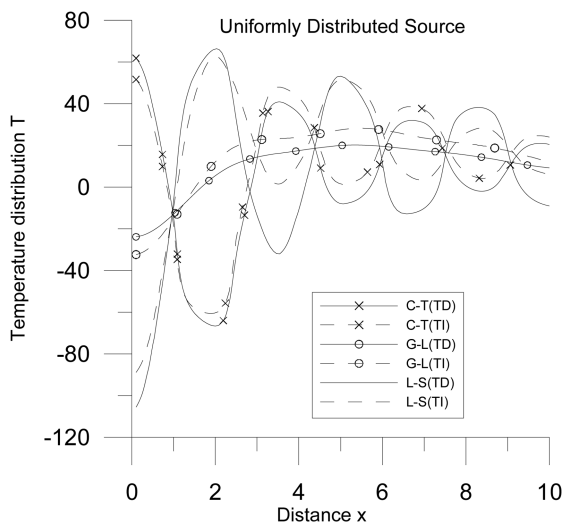


Fig. 15 Variation of temperature distribution with distance x

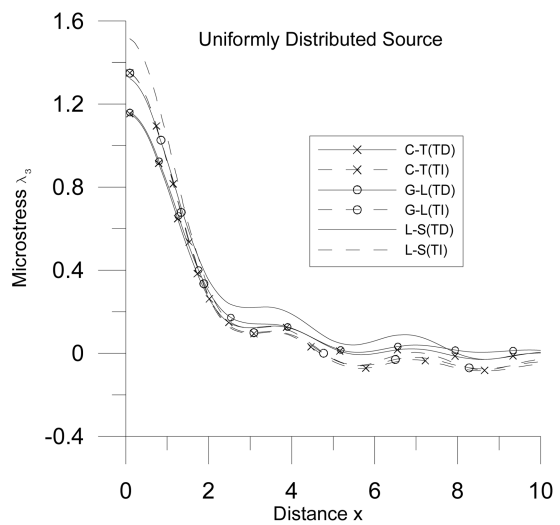


Fig. 16 Variation of microstress with distance x

shows the variation of stresses and temperature distribution on application of concentrated and uniformly distributed thermal source. Fig. 9 shows that the values of normal stress for C-T theory start with sharp initial decrease within the range $0 \leq x \leq 2$, then oscillate with decreasing amplitude for both TI and TD modulus of elasticity. While for G-L theory and for both TI and TD its values oscillate with small amplitude about origin, and in the case of L-S theory its values initially increases then, oscillate about origin with increase in distance x . Similar behavior with difference in their magnitude is observed when uniformly distributed source is applied. It is evident from Figs. 10 and 14 that the values of m_{32} increase with increase in distance x for L-S theory for both TD and TI modulus of elasticity. While for G-L and C-T theories its values start with sharp initial decrease and

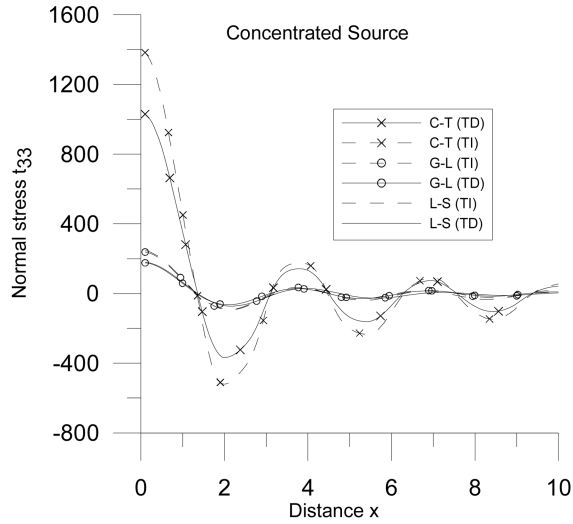


Fig. 17 Variation of normal stress with distance x

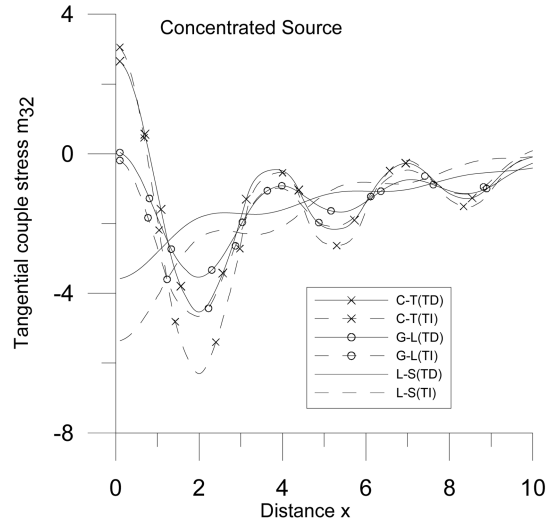


Fig. 18 Variation of tangential couple stress with distance x

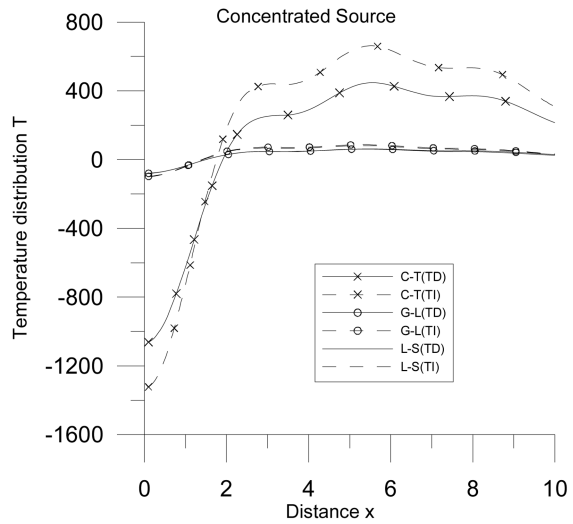


Fig. 19 Variation of Temperature Distribution T with distance x

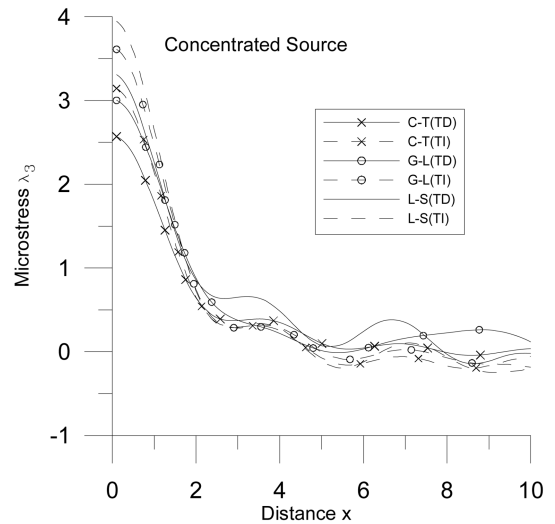


Fig. 20 Variation of microstress with distance x

oscillate with increasing magnitude. Figs. 11 and 15 shows the variation of temperature distribution T on application of concentrated and uniformly distributed thermal source. For C-T theory its values sharply decrease and then oscillate with decreasing magnitude, whereas reverse behavior is observed in the case of L-S theory. The values for G-L theory lies in between of C-T and L-S theory. It is evident from Figs. 12 and 16 that the values of microstress for all the three generalized theories decrease with increase in distance x on application of both concentrated and uniformly distributed thermal source. Figs. 17-24 show the variations of stresses and temperature distribution on application of concentrated and uniformly distributed microstress force. It is evident from Figures that the values of t_{33} on application of both concentrated and Uniformly distributed microstress force are

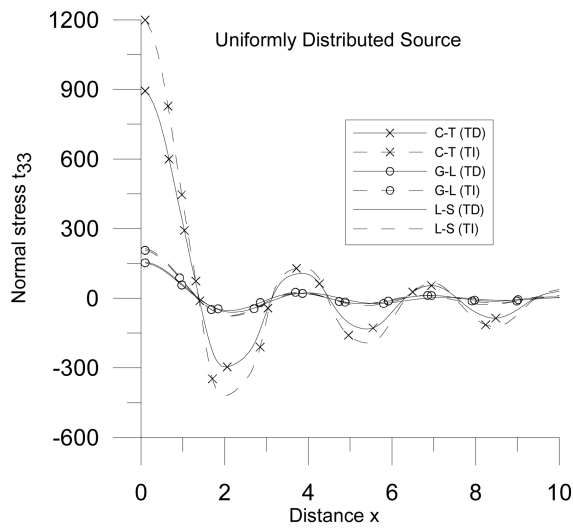


Fig. 21 Variation of normal stress with distance x

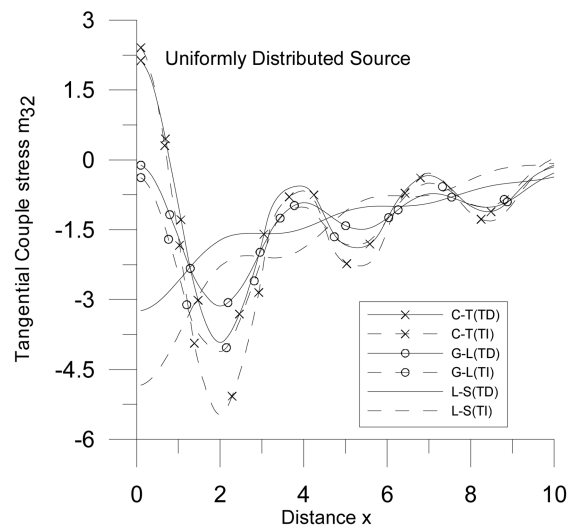


Fig. 22 Variation of tangential couple stress with distance x

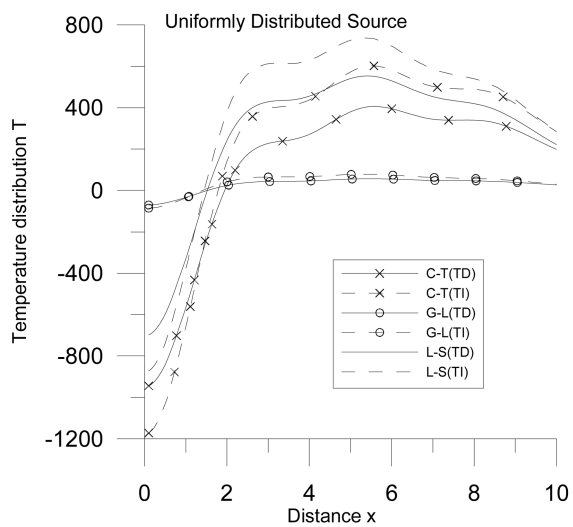


Fig. 23 Variation of temperature distribution with distance x

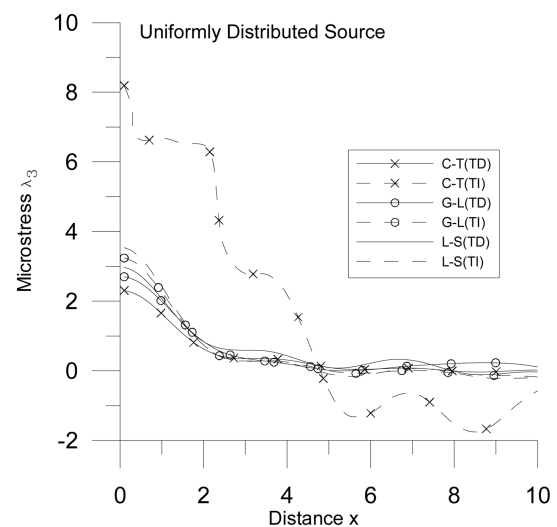


Fig. 24 Variation of microstress with distance x

similar in nature. For C-T theory its values sharply decrease and then oscillate with decreasing amplitude while for L-S and G-L they its values oscillate about origin with small amplitude. The values of m_{32} on application of microstress force is exactly same as that obtained on the application of thermal source but with the difference in their magnitude. It is evident from Figs. 19 and 23 that for L-S theory the values of temperature distribution initially increase and then became constant about origin on application of both concentrated and distributed microstress force. But for L-S and G-L theories, when concentrated microstress force is applied its value initially increases, then appears to be constant near the origin with increase in distance x , while on application of uniformly distributed microstress force its value start with sharp increase then slowly increases and afterwards

decreases with increase in x . Similar behavior in the values of microstress on application of microstress force is observed as that observed in the case of thermal source but with difference in their magnitude as shown in Figs. 20 and 24.

8. Conclusions

The results of the problem may be applied to a wide class of geophysical problems involving temperature change. The deformation at any point of the medium at any point is useful to analyze the deformation Field around mining tremors and drilling into the crust of the earth. It is observed from the figures that when concentrated mechanical force is applied, the value of normal force stress, tangential couple stress and microstress is maximum for C-T theory and minimum for L-S theory, while for G-L theory its values lie in between the value of C-T and LS, for both temperature dependent and independent material constants. Similar behavior is observed on the values of m_{32} and λ_3 when concentrated force and on temperature distribution T when uniformly distributed mechanical force is applied. However the reverse behavior on the values of t_{33} , m_{32} , λ_3 is observed when uniformly distributed force is applied and on T when concentrated force is applied. When thermal source is applied the variation pattern of m_{32} and T is observed to be opposite to that obtained on the application of mechanical force, however similar variation pattern of the values of t_{33} and λ_3 is observed. The opposite behavior for C-T and L-S theory is observed on the value of temperature distribution T when both concentrated and uniformly distributed thermal sources are applied. When microstress force is applied the values of stresses and temperature distribution behave in similar way as in the case of mechanical force.

It is clear that normal stress for L-S and G-L theory initially has increasing and then decreasing effect with the modulus of elasticity being dependent on reference temperature. While on application of thermal source its value get decreased with the modulus of elasticity being dependent on the reference temperature. The values of tangential couple stress m_{32} decreased on application of concentrated mechanical force and increased on the application of uniformly distributed mechanical force. However when thermal source is applied and for L-S and G-L its value is more for T-D than that of TI, while reverse behavior is observed in the case of C-T theory. When microstress force is applied similar behavior is observed. The value of temperature distribution T get increased in L-S theory, however for L-S and G-L initially its values get decrease and afterwards increased. The value of microstress for C-T theory get decreased while that of L-S and G-L theory get increased with the modulus of elasticity being dependent on reference temperature.

References

- Budaev, O.R., Ivanova, M.N., Damdinov, B.B. (2003), "Temperature dependence of shear elasticity of some liquids", *Adv. Colloid Interfac.*, **104**, 307-310.
- Bakshi, A., Roy, B.K. and Bera, R.K. (2007), "Effect of generalized thermoelasticity materials with memory", *Struct. Eng. Mech.*, **25**(5).
- Cicco, S. De (2003), "Stress concentration effects in microstretch elastic solids", *Int. J. Eng. Sci.*, **41**, 187-199.
- Eringen A.C. (1984), "Plane waves in non-local micropolar elasticity", *Int. J. Eng. Sci.*, **22**, 1113-1121.
- Eringen, A.C. (1999), "Microcontinuum field theories I: Foundations and solids", *Springer-Verlag*, New York.
- Ezzat, M.A., Othman, M.I. and El-Karamany, A.S. (2001), "The dependence of modulus of elasticity of reference

- temperature in generalized thermoelasticity”, *J. Therm. Stresses*, **24**, 1159-1176.
- Ezzat, M.A., El-Karamany, A.S. and Samaan, A.A. (2004), “The dependence of the modulus of elasticity on reference temperature in generalized thermoelasticity with thermal relaxation”, *Appl. Math. Comput.*, **147**, 169-189.
- Kumar, R. and Choudhary S. (2004), “Dynamical behaviour of orthotropic micropolar elastic medium”, *J. Vib. Control*, **8**, 1053-1069.
- Kumar, R. and Deshwal, S. (2000), “Disturbance due to a point source in a generalized thermomicrostretch elastic medium”, *Ganita*, **51**, 187-206.
- Kumar R. and Singh B. (1998), “Wave propagation in a generalized thermomicrostretch elastic solid”, *Int. J. Eng. Sci.*, **36**, 891-912.
- Liu X. and Hu G. (2004), “Inclusion problem of microstretch continuum”, *Int. J. Eng. Sci.*, **42**, 849-860.
- Lomarkin, V.A. (1976), “The theory of elasticity of non-homogeneous bodies”, Moscow.
- Rishin, V.V., Lyashenko, B.A., Akinin, K.G. and Nadezhdin G.N. (1973), “Temperature dependence of adhesion strength and elasticity of some heat resistant coatings”, *Strength Mat.(USSR)*, **5**, 123-126.
- Sturnin, D.V. (2001), “On characteristics times in generalized thermoelasticity”, *J. Appl. Math.*, **68**, 816-817.
- Svanadze M. (2004), “Fundamental solution of the system of equations of steady oscillations in the theory of microstretch elastic solids”, *Int. J. Eng. Sci.*, **42**, 1897-1910.
- Szueces, F., Werner, M., Sussmann R.S., Pickles, C.S.J. and Frecht M.J. (1999), “Temperature dependence of Young’s modulus and degradation of chemical vapor deposited diamond”, *J. Appl. Phys.*, **86**, 6010-6017.
- Tanigawa, T. (1995), “Some basic thermoelastic problem from nonhomogeneous structural materials”, *Appl. Mech. Rievew*, **117**, 8-16.

Appendix A

In above relations, we have used the following notations :

u_i components of displacement vector, ϕ_i component of microrotation vector, t_{ij} components of the stress tensor, m_{ij} components of the couple stress tensor, ε_{ij} components of micropolar strain tensor, satisfying

$$\varepsilon_{ij} = u_{j,i} + \varepsilon_{ij3}\phi_3.$$

$\mu, \alpha, \beta, \gamma, K, \alpha_0, \lambda_1, \lambda_0$ are material constants, ρ is the density, j is the microinertia, j_0 is the microinertia of microelements, ϕ^* is the scalar point microstretch function, λ_k is the component of microstress tensor, ε_{ijk} permutation symbol, K^* is the coefficient of thermal conductivity, C^* is specific heat at constant strain, T is the temperature change, T_0 is uniform temperature, $\nu = (3\lambda + 2\mu + K)\alpha_{01}$, $\nu_1 = (3\lambda + 2\mu + K)\alpha_{02}$, where, α_{01} and α_{02} are the coefficients of linear thermal expansion. The comma notation denotes spatial derivatives. For L-S theory, $\tau_1 = 0$, $n_0 = 1$, For G-L theory, $\tau_1 > 0$, $n_0 = 0$. The thermal relaxation times τ_0 and τ_1 satisfy the inequality $\tau_1 \geq \tau_0 > 0$ for G-L theory only. However, it has been proved by Sturnin (2001) that the inequalities are not mandatory for τ_0 and τ_1 to follow. Also for C-T theory, $\tau_0 = \tau_1 = 0$.

Appendix B

$$A = -2\xi^2 - R \frac{\rho c_1^2 p^2 \gamma_a \omega^{*2} + 2c_1^2 K_a (\mu_a + K_a) + c_1^2 K_a^2}{(\mu_a + K_a) \gamma_a \omega^{*2}},$$

$$B = \xi^4 + R \frac{\rho c_1^2 p^2}{(\mu_a + K_a)} + \frac{2c_1^2 \xi^2 K_a}{\gamma_a \omega^{*2}} + R \frac{K_a c_1^2 [2p^2 \rho c_1^2 - K_a \xi^2 - R \rho j p^2]}{\gamma_a \omega^{*2} (\mu_a + K_a)},$$

$$C = -\left[a_1 + \frac{n_1}{n_2} - n_4^2 - a_5 n_3 \right] n_2, \quad D = -[a_2 - a_1 n_1 - a_3 n_4 - a_6 n_3] n_2, \quad E = [a_2 n_2 + a_4 n_4 + a_7 n_3] n_2$$

where

$$\begin{aligned} n_1 &= (\xi^2 + R p^2), & n_2 &= \frac{\rho c_1^4}{\omega^{*2} \alpha_{oa}}, & n_3 &= (1 + \tau_1 p), & n_{4,5} &= \frac{\lambda_{oa,1a}}{\rho c_1^2}, & n_6 &= \frac{(p + n_o \tau_o p^2)}{K_a^*}, \\ a_1 &= \frac{2}{n_2} + \frac{(p + \tau_o p^2)}{n_2} + n_5 + R \frac{j_o \omega^{*2} p^2}{2 c_1^2}, & a_2 &= -\left(\frac{\xi^2}{n_2} + n_5 + \frac{j_o \omega^{*2} p^2}{2 c_1^2} \right) (n_1 + R \tau_o p^2) - \frac{v_{1a}^2 T_o n_3 n_6}{\rho \omega^*}, \\ a_3 &= -n_4 (\xi^2 + n_1 + R \tau_o p^2) - \frac{v_{1a} v_a T_o n_3 n_6}{\rho \omega^*}, & a_4 &= n_4 \xi^2 (n_1 + R \tau_o p^2) + \xi^2 \frac{v_{1a} v_a T_o n_1 n_6}{\rho \omega^*}, \\ a_5 &= -\frac{\omega^* \alpha_{oa} v_a^2 T_o n_6}{\rho^2 c_1^4}, & a_6 &= \frac{v_{1a} v_a T_o n_4 n_6}{\rho c_1^2 \omega^*} + \frac{2 \omega^* \alpha_{oa} \xi^2 v_a^2 T_o n_3 n_6}{\rho^2 c_1^4} + \frac{n_5 n_6 v_a^2 T_o}{\rho \omega^*} + R \frac{j_o \omega^{*2} p^2 v_a^2 T_o n_6}{2 \rho c_1^2}, \\ a_7 &= \frac{v_a^2 T_o n_6 \xi^2}{2 \rho^2 c_1^2 \omega^*} \left[2 \frac{v_{1a}}{v_a} - 2 \omega^{*2} \alpha_{oa} \frac{\xi^2}{c_1^2} - 2 \lambda_{1a} - R j_o \omega^{*2} p^2 \xi^2 \right], & R &= \frac{1}{(1 - \alpha^* T_o)} \end{aligned}$$

Appendix C

$$\begin{aligned} m_{1,2} &= \frac{(\mu_a + K_a)}{K_a} (q_{1,2}^2 - \xi^2) - R \frac{\rho c_1^2 p^2}{K_a}, & r_{3,4,5} &= \frac{a_9 q_{3,4,5}^2 + a_{10}}{c_1^2 q_{3,4,5}^2 / n_2 + a_8}, & s_{3,4,5} &= \frac{q_{3,4,5}^2 + n_4 r_{3,4,5} - n_1}{n_3}, \\ a_8 &= \frac{v_{1a} n_4}{v_a} - n_5 - \frac{j_o \omega^{*2} p^2}{c_1^4}, & a_9 &= n_4 - \frac{v_{1a}}{v_a}, & a_{10} &= -n_4 \xi^2 + \frac{v_{1a} n_1}{v_a} \end{aligned}$$

Appendix D

$$\begin{aligned} a_{1,2}^* &= q_{1,2} v \xi (n_4 - 1), & a_{3,4,5}^* &= n_4 (r_{3,4,5} - \xi^2) + q_{3,4,5}^2 - s_{3,4,5} n_3, \\ b_{1,2}^* &= \frac{(\mu_a \xi^2 + (\mu_a + K_a) q_{1,2}^2 - K_a m_{1,2})}{\rho c_1^2}, & b_{3,4,5}^* &= \frac{q_{3,4,5} v \xi (2 \mu_a + K_a)}{\rho c_1^2}, & c_{1,2}^* &= \frac{\omega^{*2} \gamma_a m_{1,2} q_{1,2}}{\rho c_1^4}, \\ c_{3,4,5}^* &= \frac{b_{oa} v \xi \omega^{*2} r_{3,4,5}}{\rho c_1^4}, & d_{1,2}^* &= \frac{b_{oa} v \xi \omega^{*2} m_{1,2}}{\rho c_1^4}, & d_{3,4,5}^* &= -\frac{\alpha_{oa} \omega^{*2} r_{3,4,5} q_{3,4,5}}{\rho c_1^4}, \end{aligned}$$

$$\Delta = \begin{vmatrix} a_1^* & a_2^* & a_3^* & a_4^* & a_5^* \\ b_1^* & b_2^* & b_3^* & b_4^* & b_5^* \\ c_1^* & c_2^* & c_3^* & c_4^* & c_5^* \\ 0 & 0 & s_3 & s_4 & s_5 \\ d_1^* & d_2^* & d_3^* & d_4^* & d_5^* \end{vmatrix} \text{ and } \Delta_i, i = 1, 2, \dots, 5 \text{ is obtained from } \Delta \text{ by interchanging } i^{\text{th}} \text{ column by the column } | P_1 P_2 P_3 P_4 P_5 |^T.$$